NSRRC - J045>0 (>014)

Research Article

SCI

Received: 3 January 2014 Revised: 24 March 2014 Accepted article published: 9 April 2014 Published online in Wiley Online Library: 23 May 2014

(wileyonlinelibrary.com) DOI 10.1002/pi.4744

Synthesis and characterization of poly(3-hexylthiophene)–poly(3-hexyloxythiophene) random copolymers with tunable band gap via Grignard metathesis polymerization

Yi-Lung Yang,[a] Yi-Huan Lee,[a,b] Yu-Ping Lee,[b] Chi-Ju Chiang,[b] Ching Shen,[b] Chun-Ching Wu,[a] Yoshihiro Ohta,[c] Tsutomu Yokozawa[c] and Chi-An Dai[a,b*]

Abstract

A series of 3-substituted polythiophene copolymers having different side chain arrangements of hexyl and hexyloxy groups has been synthesized via the Grignard metathesis (GRIM) method and systematically studied. Despite differences in monomer reactivity ratios for the nickel-catalyzed chain transfer polymerization, random sequences of hexyl- and hexyloxy-substituted polythiophenes with different monomer compositions and adjustable band-gap energies can be synthesized according to their respective comonomer feed ratio, as evidenced from NMR, UV, electrochemical measurements, and computational calculations. Structural characterization from X-ray diffraction measurements reveals that the flexible hexyloxy side chains of the monomer significantly affect the crystallinity and molecular packing of the random copolymers. This study shows potential for synthesizing random copolymers with different monomer reactivities via the GRIM method for future optoelectronic applications.

© 2014 Society of Chemical Industry

Supporting information may be found in the online version of this article.

Keywords: conducting polymer; random copolymer; XRD; P3HT; P3HOT

INTRODUCTION

π-Conjugated polymers constitute an important class of functional materials since they show potential for use in low-cost, flexible and lightweight electronic devices such as touch-screen panels,[1] solar cells,[2] field-effect transistors[3] and light-emitting diodes.[4] Recently, research geared towards finding highly efficient polymer solar cells has received tremendous amount of attention due to the ever increasing environmental concerns over carbon emissions from burning fossil fuels. Various types of conducting polymers have been synthesized and used for solar cell device fabrication.[5–7] Among them, regioregular poly(3-hexylthiophene)s (P3HTs) have been used most extensively since they are highly stable and solution-processable. Also, they show high charge mobility and power conversion efficiency. A typical solar cell device using P3HT as an active material is made by forming a so-called bulk heterojunction structure, which involved blending the polymer with various types of n-type nanoparticles, such as a C_{60} derivative of phenyl-C_{61}-butyric acid methyl ester (PCBM), titanium oxide or zinc oxide, sandwiched between an anode of typically PEDOT:PSS/ITO glass and an aluminium cathode. Currently, P3HT/PCBM-based solar cells exhibit a maximum power conversion efficiency of around 3–5%.[8]

In order to further enhance the power conversion efficiency of polymer-based solar cells, several strategies have been proposed. First, since P3HT only absorbs *ca* 20% of the solar spectrum, a higher efficiency is expected for new conducting polymers with a lower band-gap energy so as to absorb a wider range of the solar spectrum.[9] In this regard, donor–acceptor alternating conducting polymers are of particular interest since the combination of different donors and acceptors can be used to create a vast array of conducting polymers with novel properties that can be tailored for optoelectronic applications.[10] Among them, the usage of 3-alkoxythiophene monomer units for the synthesis of conducting polymers appears to be very promising. This is due to the oxygen atom in the alkoxy side chain giving the monomer unit an electron-donating ability; as opposed to a regular 3-alkylthiophene monomer unit, which may serve as an electron acceptor. Conventionally, poly(3-alkylthiophene)s (P3ATs) and poly(3-alkoxythiophene)s (P3AOTs) were synthesized through

* *Correspondence to: Chi-An Dai, Department of Chemical Engineering, National Taiwan University, Taipei, 10617 Taiwan. E-mail: polymer@ntu.edu.tw*

a *Institute of Polymer Science and Engineering, National Taiwan University, Taipei, 10617 Taiwan*

b *Department of Chemical Engineering, National Taiwan University, Taipei, 10617 Taiwan*

c *Department of Material and Life Chemistry, Kanagawa University, Yokohama 221-8686, Japan*

 © 2014 Society of Chemical Industry

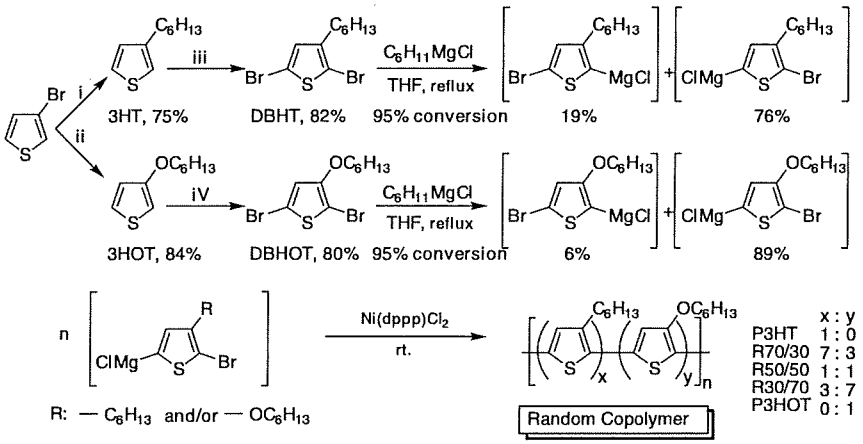

Scheme 1. Synthetic routes to monomers and polymers: (i) Mg, $Ni(dppp)Cl_2$, ether, $C_6H_{13}Br$, N_2, room temperature (rt.), 24 h; (ii) NaH, dimethylformamide, $C_6H_{13}OH$, CuBr, N_2, 110 °C, 1 h; (iii) *N*-bromosuccinimide, THF, rt., 2 h; (iv) *N*-bromosuccinimide, THF, −78 °C, 3 h.

oxidative polymerization with iron(III) chloride as the oxidizing catalyst.[11] However, these polymers synthesized using oxidative polymerization are only regiorandom in the chain structure. The regioregularity of these types of conducting polymers was later found to be critical for their optoelectronic properties,[12] their ability to form highly ordered structures[13,14] and their device performances.[15]

The first successful synthesis of regioregular P3ATs took place in 1993 by McCullough *et al.* They and Yokozawa and co-workers have further demonstrated that well-defined P3HTs can be synthesized with low polydispersity via a chain growth mechanism using a catalyst-transfer polycondensation method mediated by a nickel catalyst (Grignard metathesis (GRIM) method).[16–18] The synthesized regioregular P3ATs usually have a regioregularity of 95% or higher. The effect of regioregularity of 3-alkyl- or 3-alkoxy-substituted polythiophenes on their chromic and chiral properties has further been investigated by various groups.[19,20] However, no systematic study has been made by varying the monomer composition between alkyl and alkoxy side chains in the polythiophenes. In addition, Koeckelberghs and co-workers reported the effect of the transfer of supramolecular chirality in block copolymers of P3HT and P3AOT,[21,22] and studied the synthesis of P3HT-*block*-poly[3-(3,7-(*S*)-dimethyloctyloxy)thiophene] with different spacers.[23] However, the synthesis of random copolymers with different monomer units using the GRIM method is challenging since it has been shown that the success of catalyst-transfer polymerization depends strongly on the monomer reactivity ratio.[18]

Herein, we report that a series of P3AT-*ran*-P3AOT copolymers having a random sequence of hexyl and hexyloxy chains as the substituents can be successfully synthesized via the GRIM method mediated by a nickel catalyst, Ni(1,3-bis(diphenylphosphino) propane)Cl_2 (Ni(dppp)Cl_2).[24–27] Poly(3-hexylthiophene)-*ran*-poly (3-hexyloxythiophene) (P3HT-*ran*-P3HOT) with five different mole fractions were synthesized via the GRIM method. This study was motivated by the fact that both P3AT and P3AOT homopolymers have been successfully synthesized using GRIM, yet the synthesis of the random copolymers of P3AT and P3AOT with adjustable band-gap energy using GRIM has not been reported in the literature. Since the electron-donating property of the alkoxy side chain may impart to 2,5-dibromo-3-hexyloxythiophene (DBHOT) monomers a high polymerization reactivity, whether or not the random copolymerization using GRIM still follows a living chain polymerization nature is unknown from the literature. Therefore, the current study may shed light on the copolymerization of monomers with different reactivities using GRIM.

EXPERIMENTAL

Materials and equipment

2,5-Dibromo-3-hexylthiophene (DBHT)[28] and DBHOT[29] were synthesized according to known procedures from the literature using 3-hexylthiophene (3HT)[30] and 3-hexyloxythiophene (3HOT),[11] respectively. The synthetic routes and characterization of the monomers and the resulting copolymers are illustrated in Scheme 1 and Fig. S1. The detailed synthetic procedures and quenching experiments of the GRIM reaction are described in the following. The thermal properties of the polymers were determined using TGA measurements.

General method for the synthesis of P3HT and P3HOT homopolymers and P3HT-*ran*-P3HOT copolymers via GRIM

P3HT and P3HOT homopolymers and P3HT-*ran*-P3HOT copolymers were prepared by GRIM polymerization. A three-neck round-bottom flask equipped with a condenser and a funnel was flushed with nitrogen and charged with different fractions of DBHOT and DBHT (0.01 mole of the monomers). Anhydrous tetrahydrofuran (THF; 200 mL) and isopropylmagnesium chloride (2 mol L^{-1} in THF, 0.01 mol) were added to the flask via syringe. The reaction mixture was allowed to stir for 120 min at a gentle reflux (*ca* 75 °C). The catalyst, Ni(dppp)Cl_2, which was previously dissolved in anhydrous THF, was then added through the funnel into the polymerization flask as quickly as possible to ensure all initiations occurred at the same time. The reaction was allowed to proceed at room temperature for 45 min. Then, the reaction product was precipitated in methanol (CH_3OH). The polymers were filtered, and purified using Soxhlet extraction in sequence with solvents of hexanes, CH_3OH and $CHCl_3$. Finally, the residual chloroform was removed from the polymer by drying in a vacuum oven at room temperature. The final product was a dark red powder and recovered in quantitative yield. The polymers were stored under an inert atmosphere.

P3HT. ^{1}H-NMR (400 MHz, $CDCl_3$; δ, ppm): 0.92 (t, $J = 13$ Hz, 3 H), 1.35–1.54 (m, 4 H), 1.55 (m, $J = 15$ Hz, 2 H), 1.70 (m, $J = 14$ Hz, 2 H),

 © 2014 Society of Chemical Industry

2.81 (t, $J = 15$ Hz, 2 H), 7.00 (s, 1 H). $M_w = 50.3 \times 10^3$ g mol^{-1} and PDI = 1.25.

R70/30 (feed ratio of DBHT/DBHOT = 7:3). ^{1}H-NMR (400 MHz, $CDCl_3$; δ, ppm): 0.90–0.95 (m, 6 H), 1.25–1.90 (m,8 H), 2.79 (m, $J = 12$ Hz, 2.44 H), 4.17 (t, $J = 13$ Hz, 1.56 H), 6.97–6.98 (m, 2 H). $M_w = 41.3 \times 10^3$ g mol^{-1} and PDI = 1.35.

R50/50 (feed ratio of DBHT/DBHOT = 1:1). ^{1}H-NMR (400 MHz, $CDCl_3$; δ, ppm): 0.91–0.96 (m, 6 H), 1.26–1.89 (m,8 H), 2.78 (m, $J = 12$ Hz,1.72 H), 4.16 (t, $J = 13$ Hz, 2.28 H), 6.96–6.99 (m, 2 H). $M_w = 35.3 \times 10^3$ g mol^{-1} and PDI = 1.52.

R30/70 (feed ratio of DBHT/DBHOT = 3:7). ^{1}H-NMR (400 MHz, $CDCl_3$; δ, ppm): 0.90–0.92 (m, 6 H), 1.26–1.89 (m,8 H), 2.77 (m, $J = 12$ Hz, 0.76 H), 4.15 (t, $J = 13$ Hz, 3.24 H), 6.92–6.99 (m, 2 H). $M_w = 16.0 \times 10^3$ g mol^{-1} and PDI = 1.55.

P3HOT. ^{1}H-NMR (400 MHz, $CDCl_3$; δ, ppm): 0.91 (t, $J = 14$ Hz, 3 H), 1.23–1.54 (m,6 H), 1.86 (m, $J = 14$ Hz, 2 H), 4.14 (t, $J = 13$ Hz, 2 H), 6.88 (s, 1 H). $M_w = 10.5 \times 10^3$ g mol^{-1} and PDI = 1.64.

Quenching experiment of GRIM reaction of DBHT

A three-neck round-bottom flask equipped with a condenser and a funnel was flushed with nitrogen and charged with DBHT (0.652 g, 2.00 mmol). Anhydrous THF (20 mL) and 2.00 mmol of isopropylmagnesium chloride were added to the flask via a syringe. The reaction mixture was allowed to stir for 1.5 h at a gentle reflux (*ca* 75 °C) and then quenched with trimethylsilyl chloride (TMS-Cl) at −40 °C for 2.0 h. Finally, we examine the chemical shift of the proton on the thiophene ring with ^{1}H-NMR to calculate the amount of DBHT (6.77 ppm, 5%), 2-bromo-4-hexyl-5-TMS thiophene (6.87 ppm, 19%) and 2-bromo-3-hexyl-5-TMS thiophene (6.79 ppm, 76%).

Quenching experiment of GRIM reaction of DBHOT

A three-neck round-bottom flask equipped with a condenser and a funnel was flushed with nitrogen and charged with DBHOT (0.684 g, 2.00 mmol). Anhydrous THF (20 mL) and 2.00 mmol of isopropylmagnesium chloride were added to the flask via a syringe. The reaction mixture was allowed to stir for 1.5 h at gentle reflux (*ca* 75 °C) and then quenched with TMS-Cl at −40 °C for 2.0 h. Finally, we examine the chemical shift of the ^{1}H NMR signals of the protons on the thiophene ring to calculate the amount of DBHOT (6.75 ppm, 5%), 2-bromo-4-hexyloxy-5-TMS thiophene (6.88 ppm, 6%) and 2-bromo-3-hexyloxy-5-TMS thiophene (6.84 ppm, 89%).

RESULTS AND DISCUSSION

Synthesis of P3HT-*ran*-P3HOT random copolymers

P3HT and P3HOT homopolymers and P3HT-*ran*-P3HOT copolymers were synthesized via the GRIM method. In order to investigate the properties of the copolymers on an equal basis, we changed the DBHT/DBHOT comonomer compositions, but fixed the molar ratio of the total comonomer amount to nickel catalyst in order to get a similar theoretical molecular weight of the synthesized polymers. First, we fixed the number of moles of the starting comonomers (DBHT and DBHOT), [M], and nickel catalyst, [I], at 10.0 and 0.02 mmol, respectively, in 200 mL of THF for a theoretical degree of polymerization equal to 500. Then, we changed the comonomer compositions to synthesize five different P3HT-*ran*-P3HOT copolymers. The feed DBHT/DBHOT molar ratios were 1.0, 0.7, 0.5, 0.3, to 0.0, denoted as P3HT, R70/30, R50/50, R30/70, and P3HOT, respectively. These polymers were synthesized under the same reaction conditions, with the catalyst and reagents being completely dissolved in anhydrous THF. The resulting products were analyzed using ^{1}H-NMR spectroscopy and gel permeation chromatography (GPC). The molecular weight data for these polymers are listed in Tables 1 and S1.

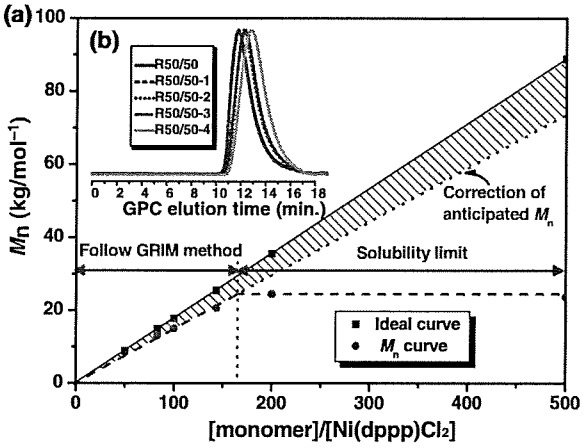

Figure 1. (a) Relationship between M_n and [monomer]/[Ni(dppp)Cl_2] ratio for the R50/50 system. (b) GPC traces of R50/50 with different molar ratios of nickel catalyst.

Table 1. Polymerization of 3HT and 3HOT using the GRIM method

Copolymer	DBHT (mol)	DBHOT (mol)	[I]/[M] (%)[a]	M_n (kg · mol^{-1})[b]	PDI[b]	Composition molar ratio of P3HT (%)[c]
P3HT	0.01	0	0.2	40.2	1.25	1.00
R70/30	0.007	0.003	0.2	30.6	1.35	0.61
R50/50	0.005	0.005	0.2	23.2	1.52	0.43
R50/50-1	0.005	0.005	0.5	22.0	1.45	0.43
R50/50-2	0.005	0.005	0.7	20.5	1.47	0.43
R50/50-3	0.005	0.005	1.0	16.5	1.46	0.43
R50/50-4	0.005	0.005	1.2	14.4	1.45	0.43
R30/70	0.003	0.007	0.2	10.3	1.55	0.19
P3HOT	0	0.01	0.2	6.4	1.64	0

[a] Molar ratio.
[b] From GPC.
[c] Via ^{1}H NMR in $CDCl_3$.

 © 2014 Society of Chemical Industry

Copolymerization of DBHT and DBHOT

In order to understand the polymerization procedure for the P3HT-*ran*-P3HOT system, the P3HT-*ran*-P3HOT copolymers were synthesized with equal moles of DBHT and DBHOT, designated as R50/50, by adding different molar ratios of the comonomers to the nickel catalyst ([M]/[I] = 83, 100, 143, 200 and 500). The relationship between the resulting number-average molecular weight (M_n) and the molar percentage of Ni catalyst for the R50/50 system is shown in Fig. 1. The linear increase in M_n of R50/50 basically follows the GRIM procedure of a chain-growth polymerization for M_n lower than 24.4 kg mol^{-1} (Fig. 1). However, the actual slope of M_n *versus* the corresponding [monomer]/[Ni(dppp)Cl$_2$] ratio does not agree with the theoretical slope, which assumes all monomers are consumed. Such a difference in molecular weights might be due to the formation of two isomers, 3-alkyl-5-bromo-2-chloromagnesiothiophene (3-Alk-5-Br-2-MgCl-Th) and 3-alkyl-2-bromo-5-chloromagnesiothiophene (3-Alk-2-Br-5-MgCl-Th), during the GRIM reaction. Due to the significant steric hindrance effect of the alkyl or alkoxy side chain, it has been reported that 3-Alk-5-Br-2-MgCl-Th monomers are not reactive during GRIM polymerization using Ni(dppp)Cl$_2$. Therefore, this intermediate monomer could not react, and the actual molecular weight would be lower than the theoretical molecular weight.

Furthermore, the ratios of the amount of 3-Alk-5-Br-2-MgCl-Th and 3-Alk-2-Br-5-MgCl-Th formed are confirmed by a separate quenching experiment, the results of which are in Table S2. The quenching results show that the percentages of 2-Br-5-MgCl-3-HT and 2-Br-5-MgCl-3-HOT within their respective isomers are 76 and 89%, respectively. This result correlates well with the corresponding deviation for M_n less than 24.4 kg mol^{-1} for R50/50. However, even as we increased the molar ratio of the comonomers to Ni(dppp)Cl$_2$ to 500 for the synthesis of theoretically higher M_n of R50/50, the resulting molecular weight of R50/50 remained nearly constant at around 24.4 kg mol^{-1}. Consequently, there appears to be an upper limit to the molecular weight for the synthesized R50/50. Therefore, the growth of P3HT-*ran*-P3HOT copolymer system can be divided into two regions. The first region represents the 'GRIM-obeyed region' and the other is the 'solubility-limited region'. In the GRIM-obeyed region, the copolymerization follows the Ni-catalyst-transfer chain-growth procedure, and the molecular weight can be correlated linearly with the molar ratios of comonomers to catalyst. In the solubility-limited region, the molecular weights are limited by the solubility of the copolymer, which depends on its composition. Koeckelberghs and co-workers also reported that the catalyst dissociates from the polymer backbone and that the number of propagations that occur before dissociation depends on the molar ratio of 3HOT monomer.[20–23]

We repeated this experiment with different feed ratios of the starting comonomers (Table 1), and the obtained results show a similar trend in that there is a respective upper limit to the M_n of the synthesized copolymer with different compositions. Figure 1 shows the relationship between the mole percentage of Ni(dppp)Cl$_2$ and the resulting M_n. According to the GPC data, the molecular weight appears to be limited by the solubility of the copolymer. The maximum M_n of R70/30, R50/50, R30/70 and P3HOT can be obtained for molar ratios of the comonomer to Ni(dppp)Cl$_2$ higher than 210, 165, 70 and 40, respectively (Table S1). The GRIM-obeyed region becomes smaller and the solubility-limited region becomes larger as the composition of 3HOT monomers is increased in the P3HT-*ran*-P3HOT system.

Comparing the behavior of monomers in copolymerization

As discussed previously, in the low-molecular-weight region, the P3HT-*ran*-P3HOT copolymers obey the GRIM chain growth

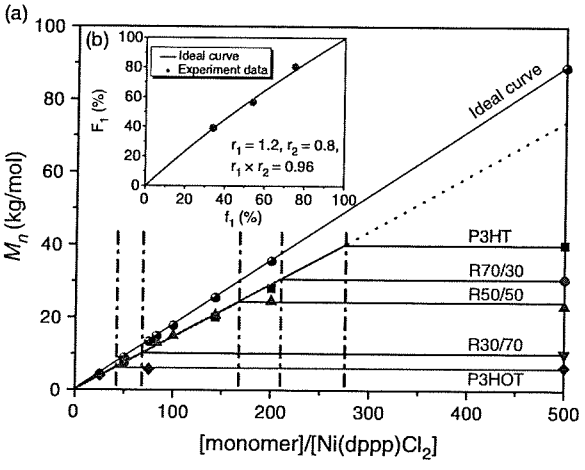

Figure 2. (a) Relationship between M_n and [monomer]/[Ni(dppp)Cl$_2$] ratio in P3HT–P3HOT system. (b) Relationship of the molar fraction of 3HOT in comonomer feed (f_1) and the molar fraction of 3HOT in copolymer (F_1).

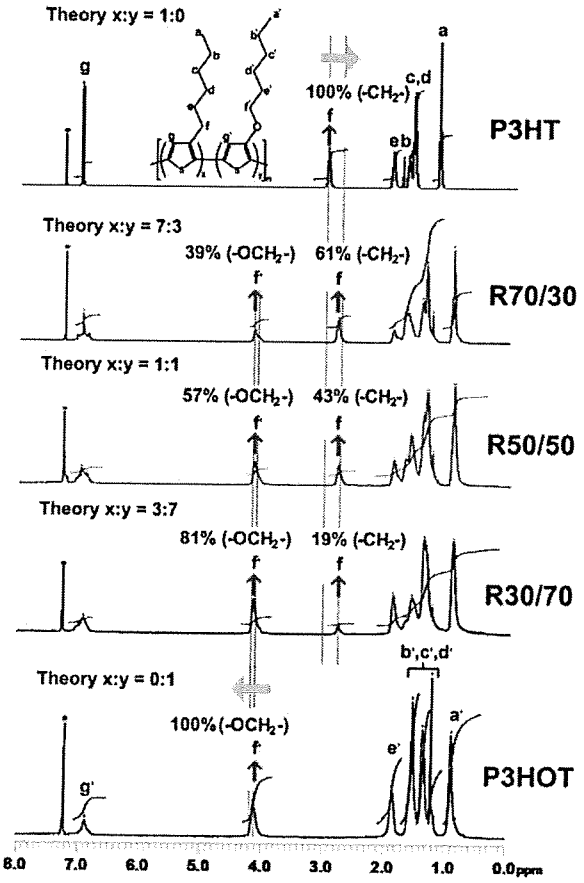

Figure 3. ^{1}H NMR spectra of polymers P3HT, R70/30, R50/50, R70/50 and P3HOT in CDCl$_3$.

© 2014 Society of Chemical Industry

rule. Thus, the monomer reactivity ratios of DBHT and DBHOT of this region can be calculated using the Mayo–Lewis equation as follows:[31]

$$F_1 = \frac{r_1 f_1^2 + f_1 f_2}{r_1 f_1^2 + 2 f_1 f_2 + r_2 f_2^2}$$

where r is the reactivity ratio, f_1 and f_2 are the mole fractions of monomers M_1 and M_2 in the feed, respectively; and F_1 is the mole fraction of M_1 in the copolymer. This equation assumes that the reactivity of the propagating species is dependent only on the monomer unit at the end of the chain. Here we define 3HOT and 3HT as species 1 and 2, respectively. The experimental data of copolymer R50/50 are used to calculate r_1 and r_2, which are found to be 1.2 and 0.8, respectively. In our case, the value of $r_1 \times r_2$ for the R50/50 system is equal to 0.96 (Fig. 2). Hence, we know that P3HT-*ran*-P3HOT copolymerization is a nearly random copolymerization based on the experimental data and the copolymerization equation.[32] Figure 2(a) shows the relationship between the derived M_n and [monomer]/[Ni(dppp)Cl_2] ratio for the P3HT-*ran*-P3HOT system. Through variation of the monomer/catalyst ratio, the M_n *versus* [M]/[I] plot shows a nonlinear dependence of M_n, which initially increases but levels off at higher feed ratios of monomer.[33] However, the molecular weight limit can be promoted by introducing 3HT segments into the polymer chain as well as improving the solubility of the resulting polymers, leading to a progressive shift towards large M_n and narrow polydispersity.

Alternatively, the compositions of 3HT and 3HOT in the copolymers were measured using ^{1}H NMR spectroscopy (Fig. 3). The ^{1}H NMR spectrum of each copolymer shows one sharp peak at around 4.14 ppm, which corresponds to the $-OCH_2-$ group of 3HOT, and another peak at around 2.77 ppm corresponding to the $-CH_2-$ group of 3HT. By increasing the molar ratio of 3HOT, the signal of the $-CH_2-$ group of 3HT at 2.81 ppm shifts to 2.77 ppm, and that of the $-OCH_2-$ group of 3HOT at 4.17 ppm shifts to 4.14 ppm. These findings clearly indicate the upfield and shielded shifts caused by the electron-donating effect of the oxygen atom and the variations in the sequence distribution of the 3HT and 3HOT repeat units. Finally, P3HT-*ran*-P3HOT is successfully defined as a random copolymer by the progressive shift of the ^{1}H NMR data.

Furthermore, by comparing the integrated areas of these two peaks, the mole fraction of 3HT and 3HOT units in P3HT-*ran*-P3HOT can be estimated. According to the integration, the actual 3HOT composition in the copolymer is a little higher (9–11%) than that of the original comonomer feed, indicating that 3HOT is slightly more reactive. The molecular weights of all polymers were determined using GPC with polystyrene as the standard. Notably, the synthesis of P3HT homopolymer has been well reported to be a nickel catalyst-transfer chain-growth polymerization (GRIM method) by which one nickel catalyst produces one living copolymer chain. Based on the above GPC results, however, the synthesis of P3HT-*ran*-P3HOT copolymers does not appear to strictly follow

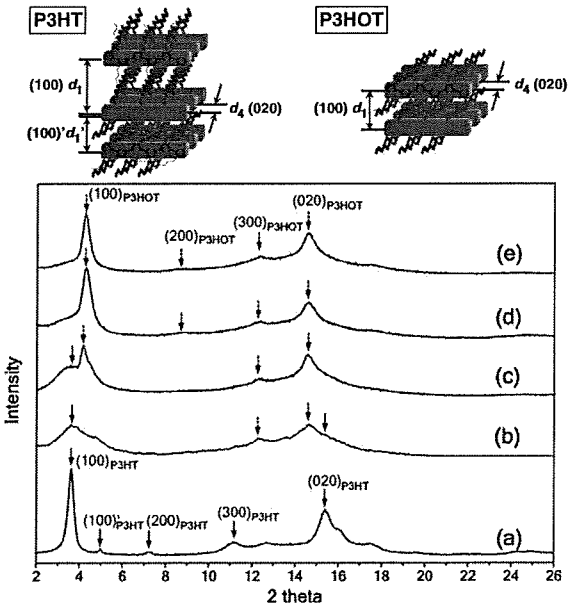

Figure 4. Powder XRD patterns of (a) P3HT, (b) R70/30, (c) R50/50, (d) R30/70 and (e) P3HOT at room temperature.

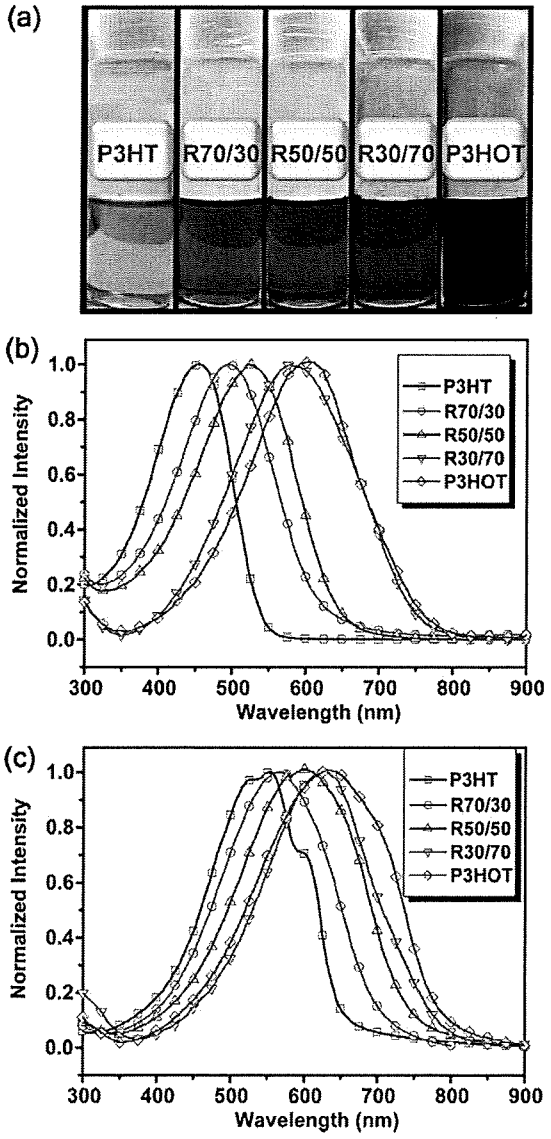

Figure 5. (a) Solution appearance of copolymers in 10^{-5} mol L^{-1} chloroform. The UV-visible absorption spectra of copolymers (b) in 10^{-5} mol L^{-1} chloroform and (c) in the film state.

© 2014 Society of Chemical Industry

the GRIM theory since the molecular weights of the copolymers differ significantly from the theoretical value.

Crystalline structure of P3HT-*ran*-P3HOT random copolymers

Solid-state thin-film samples of P3HT-*ran*-P3HOT copolymers, made by solvent-casting in chloroform (1 wt%), were selected for further structural study. The powder XRD pattern of pure P3HT has been reported by McCullough and co-workers.[34] However, the crystalline structure of random polythiophene copolymers with different substituted side chains has not been thoroughly studied yet. The XRD patterns for P3HT-*ran*-P3HOT copolymers are shown in Fig. 4 and compared with those of the homopolymers, P3HT and P3HOT.[35] Not only does P3HT exhibit a typical well-ordered crystalline structure, but P3HOT homopolymer also exhibits several sharp powder XRD peaks at $d_1 = 12.7$ Å, $d_2 = 6.73$ Å, $d_3 = 4.75$ Å and $d_4 = 3.95$ Å, revealing that P3HOT forms a highly crystalline ordered structure as well. In the small-angle region, the diffraction peaks at 4.50°, 8.51° and 12.1° are typically assigned to the first (100), second (200) and third (300) reflections of the distances between the P3HOT backbone separated by the side chains. In the wide-angle region, the peak at 14.6° (020) is considered to represent the distance between the P3HOT coplanar π-conjugated main chains.

Additionally, the other polymers also show the self-oriented lamellar structures. XRD patterns show that the interlayer d_1-spacing progressively decreases from 16.9, 16.8, 16.3 to 13.0 Å for P3HT, R70/30, R50/50 and R30/70, respectively. Since the alkoxy group has a higher flexibility than the alkyl group, the alkoxy side chain may tend towards the polymer backbone. Accordingly, the distance of the P3HOT main-chain backbone is limited by the separation of the side chain. Therefore, as we increase the mole fraction of 3HOT in the P3HT-*ran*-P3HOT system there is a decrease in the interlayer d_1-spacing, shorter than the distance for P3HT. In the meantime, the increase in full width at half maximum (FWHM) of the diffraction peaks and the corresponding reduction in P3HOT grain sizes are due to the electron-donating property of the alkoxy side chains. Moreover, the lower diffraction peak intensity of the $(100)_{P3HT}$ reflection for R50/50 indicates a decrease in crystallinity compared to that of the $(100)_{P3HOT}$ reflection for R50/50. Notably, the diffraction intensity of the $(100)_{P3HT}$ reflection for R30/70 is much reduced compared to that for P3HT.

Furthermore, the layer-to-layer π-stacking distance for P3HOT (3.95 Å) is a little larger than that for P3HT (3.76 Å). It may be that the oxygen atoms of P3HOT increase the steric hindrance, thereby preventing a close packing of the main chain. In addition, P3HT shows a small diffraction peak at 5.00°, which suggests a short interlayer $d_1'(001)'$-spacing of 11.43 Å (at 5.00°). As discussed previously, all the solution-cast P3HT-P3HOT random copolymers exhibit a crystalline structure corresponding to that of the copolymer with the major comonomer present in the chain.

Table 2. Characteristics of five different molar fractions of P3HT–P3HOT

	Absorption spectra				Cyclic voltammetry		
Copolymer	λ_{max} (nm)[a]	λ_{max} (nm)[a]	λ_{onset} (nm)[b]	E_g (eV)[c]	E_{HOMO} (eV)[d]	E_{LUMO} (eV)[e]	T_d (°C)[f]
P3HT	452	551	693	1.94	−5.27	−3.33	440
R70/30	495	568	690	1.80	−5.08	−3.28	360
R50/50	522	602	730	1.70	−4.82	−3.12	340
R30/70	579	627	765	1.62	−4.71	−3.09	330
P3HOT	601	643	784	1.58	−4.56	−2.98	270

[a] Measured in chloroform solution.
[b] Films cast from chloroform solution.
[c] Band gap estimated from the onset wavelength of optical absorption.
[d] From equation.
[e] LUMO = HOMO + E_g.
[f] Temperature at 5% weight loss under nitrogen.

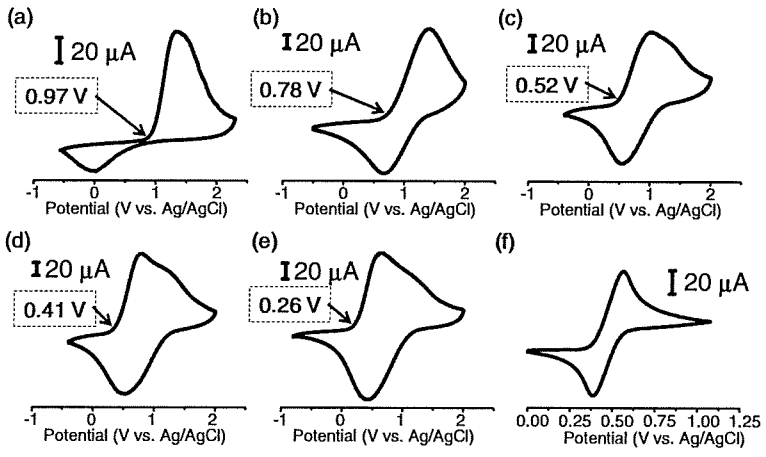

Figure 6. Cyclic voltammograms of polymers (a) P3HT, (b) R70/30, (c) R50/50, (d) R70/50 and (e) P3HOT, and (f) ferrocene standard.

 © 2014 Society of Chemical Industry

Consequently, in order to understand the origin of this result, we further investigated the optoelectronic properties of these polymers in the following section.

Photophysical and electrochemical properties

The appearance of the P3HT-*ran*-P3HOT copolymers is orange for P3HT, berry red for R70/30, purple for R50/50, and distinct color changes visually in chloroform solution, which are blue for R30/70 and dark blue for P3HOT. The UV-visible absorption of the random copolymers was measured both in a dilute chloroform solution and in a thin-film state obtained with a spin-coating process on glass. The spectra are shown in Fig. 5, while the spectral data for solution condition and thin-film form are summarized in Table 2. As the amount of 3HOT incorporated in the copolymer increases, the absorption peak is red-shifted, with the amount of shift being directly proportional to the mole fraction of 3HOT in the copolymers. The absorption maximum of homopolymer P3HOT is approximately 150 nm red-shifted compared to that of homopolymer P3HT in dilute chloroform solution, and it is 90 nm red-shifted for the thin-film state.

The energy band gap (E_g) can be calculated from the UV-visible onset point. The band-gap properties of these polymers are listed in Table 2. The band-gap energies are inversely proportional to the mole fraction of 3HOT in the P3HT-*ran*-P3HOT system. The band-gap energy of homopolymer P3HOT is 1.58 eV, which is significantly lower than that of homopolymer P3HT ($E_g = 1.94$ eV). The highest occupied molecular orbital (HOMO) can be determined by cyclic voltammetry as shown in Fig. 6. The polymers were coated onto platinum work electrodes, and measured in a 0.1 mol L^{-1} tetrabutylammonium perchlorate solution in acetonitrile. The scan rate was 100 mV s^{-1}, and the onset oxidation potentials (E_{ox}) of P3HT, R70/30, R50/50, R30/70 and P3HOT are 0.97, 0.77, 0.52, 0.40 and 0.25 eV, respectively. The oxidative potential becomes smaller when the amount of alkoxy groups increases in the polymer. The HOMO level can be calculated using the following equation:

$$E_{HOMO} = -e\left(E_{onset}^{ox,polymer} - E_{1/2}^{ox,ferrocene}\right) + (-4.8\ \text{eV})$$

The calculated HOMO value of P3HOT is −4.56 eV, which is higher than that of P3HT of −5.27 eV. The reason could be that the presence of the hexyloxy group intensifies the electron-donating property of the polymer, making it more oxidizable. Consequently, the oxidation potential decreases, and the HOMO level increases when the fraction of alkoxy side chains in the P3HT-*ran*-P3HOT system increases. This result coincides with other reports.[36] Furthermore, the lowest unoccupied molecular orbital (LUMO) level of P3HOT is calculated to be −3.33 eV, which is a little higher than the calculated value of P3HT (−2.98 eV). Notably, compared to the LUMO, the changes of the HOMO level in the P3HT-*ran*-P3HOT system are obvious. The additional alkoxy group affects the HOMO level more than the LUMO level because the oxygen atom provides more free electrons from its lone-pair electrons, which makes the electro-donating property predominate over the electron-withdrawing property.

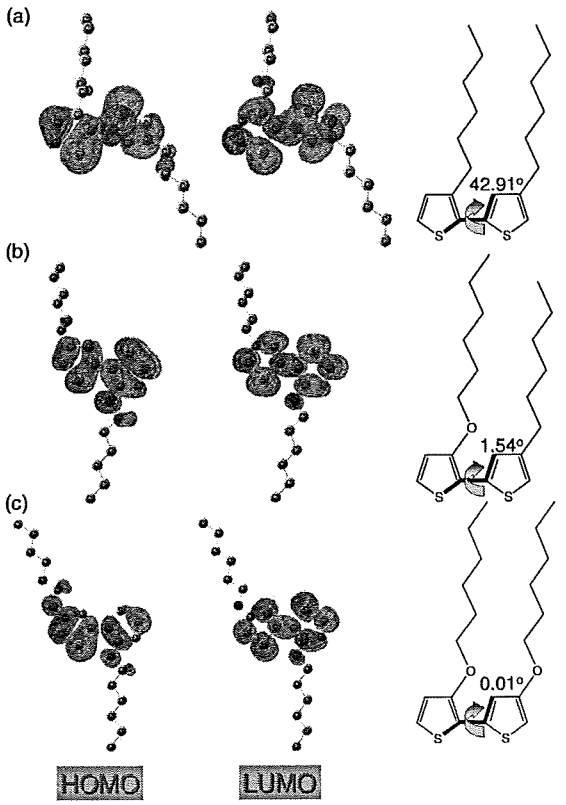

Figure 7. Molecular orbital isosurfaces of HOMO and LUMO of (a) 3HT–3HT, (b) 3HT–3HOT and (c) 3HOT–3HOT, calculated at the DFT B3LYP/6-31G* level.

Theoretical calculations

The ground-state geometries of P3HT and/or P3HOT dimers were fully optimized using the density functional theory (DFT), with B3LYP/6-31G(d), as implemented in Gaussian 03.[37] The standard DFT/B3LYP/6-31G* model used in DFT calculation has been found to be an accurate method for calculating the optimal geometry and electronic structures of many molecular systems. The HOMO and LUMO of all dimers are localized predominantly on the thiophene rings, as shown in Fig. 7. For all dimers, there is antibonding between the bridge atoms and there is bonding between the bridge carbon atom and its conjointing atoms in the same thiophenes for the HOMO level. In contrast, there is bonding in the bridge single bond and antibonding between the bridge atom and its neighbor in the same thiophene ring for the LUMO level. The electronic cloud distribution in the HOMOs of 3HOT–3HT is similar to that of 3HT–3HT on the thiophene ring. However, the electronic cloud on the side chain for 3HT is distributed less than that for 3HOT. 3HOT–3HOT has more electronic cloud distributed in the thiophene ring compared with 3HT–3HT based on the calculations. For these polymers, this implies the longest conjugation length in P3HOT compared with P3HT and the other copolymers.

CONCLUSIONS

P3HT-*ran*-P3HOT random copolymers of various molar ratios were successfully synthesized using the GRIM method. Their compositions and structures were confirmed using ^{1}H NMR analysis. Notably, due to the effect of solubility, the chain-growth phenomenon occurred only below certain critical molecular weights, which depended on the composition of the copolymers. In the P3HT-*ran*-P3HOT system, the empirical ratios of 3HOT incorporated in the copolymers were always 9–11% higher than the molar

 © 2014 Society of Chemical Industry

fraction of 3HOT in the feed because the 3HOT formed a more reactive Grignard intermediate than 3HT. The calculated reactivity data showed that the copolymerization of the P3HT-*ran*-P3HOT system is a nearly random process.

ACKNOWLEDGEMENTS

The financial support of this work from the National Science Council of Taiwan is greatly appreciated. The authors also thank all beamline staff and technical supports at the National Synchrotron Radiation Research Center of Taiwan for the X-ray measurements.

SUPPORTING INFORMATION

Supporting information may be found in the online version of this article.

REFERENCES

1 Bae S, Kim H, Lee Y, Xu XF, Park JS, Zheng Y *et al.*, *Nature Nanotechnol* **5**:574 (2010).
2 Heeger AJ, *Chem Soc Rev* **39**:2354 (2010).
3 Wang CL, Dong HL, Hu WP, Liu YQ and Zhu DB, *Chem Rev* **112**:2208 (2012).
4 Grimsdale AC, Chan KL, Martin RE, Jokisz PG and Holmes AB, *Chem Rev* **109**:897 (2009).
5 Li G, Zhu R and Yang Y, *Nature Photon* **6**:153 (2012).
6 Chochos CL and Choulis SA, *Prog Polym Sci* **36**:1326 (2011).
7 Chen J-Y and Hsu C-S, *Polym Chem* **2**:2707 (2011).
8 Ameri T, Khoram P, Min J and Brabec CJ, *Adv Mater* **25**:4245 (2013).
9 Li N, Baran D, Forberich K, Machui F, Ameri T, Turbiez M *et al.*, *Energy Environ Sci* **6**:3407 (2013).
10 Yang Y-L, Lee Y-H, Chang C-J, Lu A-J, Hsu W-C, Wang L *et al.*, *J Polym Sci A: Polym Chem* **48**:1607 (2010).
11 Chen S-A and Tsai C-C, *Macromolecules* **26**:2234 (1993).
12 Daoust G and Leclerc M, *Macromolecules* **24**:455 (1991).
13 Roux C and Leclerc M, *Macromolecules* **25**:2141 (1992).
14 Leclerc M and Daoust G, *J Chem Soc, Chem Commun 273* (1990).
15 Faid K, Frechette M, Ranger M, Mazerolle L, Levesque I, Leclerc M *et al.*, *Chem Mater* **7**:1390 (1995).
16 Miyakoshi R, Yokoyama A and Yokozawa T, *J Am Chem Soc* **127**:17542 (2005).
17 Iovu MC, Sheina EE, Gil RR and McCullough RD, *Macromolecules* **38**:8649 (2005).
18 Miyakoshi R, Yokoyama A and Yokozawa T, *Chem Lett* **37**:1022 (2008).
19 Levesque I and Leclerc M, *Chem Mater* **8**:2843 (1996).
20 Koeckelberghs G, Vangheluwe M, Samyn C, Persoons A and Verbiest T, *Macromolecules* **38**:5554 (2005).
21 Van den Bergh K, Willot P, Cornelis D, Verbiest T and Koeckelberghs G, *Macromolecules* **44**:728 (2011).
22 Van den Bergh K, Huybrechts J, Verbiest T and Koeckelberghs G, *Chem Eur J* **14**:9122 (2008).
23 Smeets A, Willot P, De Winter J, Gerbaux P, Verbiest T and Koeckelberghs G, *Macromolecules* **44**:6017 (2011).
24 Dai C-A, Yen W-C, Lee Y-H, Ho C-C and Su W-F, *J Am Chem Soc* **129**:11036 (2007).
25 Lee Y-H, Yen W-C, Su W-F and Dai C-A, *Soft Matter* **7**:10429 (2011).
26 Lee Y-H, Chang C-J, Kao C-J and Dai C-A, *Langmuir* **26**:4196 (2010).
27 Yen W-C, Lee Y-H, Lin J-F, Dai C-A, Jeng U-S and Su W-F, *Langmuir* **27**:109 (2011).
28 Chen TA, Wu XM and Rieke RD, *J Am Chem Soc* **117**:233 (1995).
29 Sheina EE, Khersonsky SM, Jones EG and McCullough RD, *Chem Mater* **17**:3317 (2005).
30 Tamao K, Kodama S, Nakajima I, Kumada M, Minato A and Suzuki K, *Tetrahedron* **38**:3347 (1982).
31 Mayo FR and Lewis FM, *J Am Chem Soc* **66**:1594 (1944).
32 Odian G, *Principles of Polymerization*, 4th edition. Wiley, Hoboken, NJ (2004).
33 Koeckelberghs G, Vangheluwe M, Van Doorsselaere K, Robijns E, Persoons A and Verbiest T, *Macromol Rapid Commun* **27**:1920 (2006).
34 McCullough RD, Tristram-Nagle S, Williams SP, Lowe RD and Jayaraman M, *J Am Chem Soc* **115**:4910 (1993).
35 Chen SA and Ni JM, *Macromolecules* **25**:6081 (1992).
36 Hu X and Xu LG, *Polymer* **41**:9147 (2000).
37 Frisch MJ, Trucks GW, Schlegel HB, Scuseria GE, Robb MA, Cheeseman JR *et al.*, Gaussian, Inc., Wallingford CT, (2004).

 © 2014 Society of Chemical Industry